IEEE Access
Multidisciplinary | Rapid Review | Open Access Journal

Received March 10, 2021, accepted March 24, 2021, date of publication April 9, 2021, date of current version April 19, 2021.

*Digital Object Identifier 10.1109/ACCESS.2021.3072059*

# Resource Allocation for LEO Beam-Hopping Satellites in a Spectrum Sharing Scenario

**JINGYU TANG, DONGMING BIAN, GUANGXIA LI, JING HU, AND JIAN CHENG**
College of Communications Engineering, Army Engineering University of PLA, Nanjing 210007, China
Corresponding author: Dongming Bian (biandm_satlab@163.com)

**ABSTRACT** In recent years, low earth orbit (LEO) satellite constellation systems have been developed rapidly. However, the scarcity of satellite spectrum resources has become one of the major obstacles to this trend. LEO satellite constellation communication systems sharing the spectrum of incumbent geostationary earth orbit (GEO) satellite system is a feasible way to alleviate spectrum scarcity. Therefore, it has practical significance to study the optimization of satellite resources allocation (RA) in a spectrum sharing scenario. This paper focuses on the RA problem that LEO satellites share a GEO high throughput satellite's spectrum in a beam-hopping (BH) manner. The GEO satellite system is served as the primary system and the LEO satellite constellation system is served as the secondary system whose frequency bands and transmitting power are strictly limited. Compared with conventional multibeam satellites, BH satellites have the advantage of flexibility in the time dimension. Therefore, we make full use of the flexibility of LEO BH satellites to realize the matching of traffic demand and traffic supply. The RA problem is decomposed into three sub-problems, namely, frequency band selection (FBS) problem, illuminated cell selection (ICS) problem, and transmitting power allocation (TPA) problem. We solve each sub-problem in order and finally form a complete RA scheme. The performance evaluation of the proposed RA scheme is carried out in real-time and simulation results show that the LEO BH satellite paired with the RA scheme we proposed has good adaptability to the uneven distribution of traffic demand in the spectrum sharing scenario.

**INDEX TERMS** LEO satellite constellation, GEO satellite system, spectrum sharing, beam-hopping, resource allocation.

## I. INTRODUCTION

Low earth orbit (LEO) satellite constellation systems, such as OneWeb [1], SpaceX [2], and Telesat [3] systems, can provide broadband Internet access services for areas with underdeveloped telecommunication infrastructure. Many satellite-related companies have put forward their own LEO satellite constellation plans. However, the rapid development of LEO satellite constellation systems intensifies the competition of spectrum resources. To break through the bottleneck of spectrum scarcity, on the one hand, higher frequency bands from Ka to Q/V band can be developed; on the other hand, improving spectrum utilization is a more feasible option at present. The cognitive radio (CR) technology can sense the available spectrum of the surrounding environment and use idle spectrum resources in an opportunistic manner. Based on CR technology, cognitive satellite communications allow a satellite communication system to utilize another communication system's spectrum resources with an acceptable interference level. According to the type of sharing systems, cognitive satellite communications can be mainly divided into three categories: *a)* spectrum sharing between the satellite communication system and the terrestrial communication system [4], [5], *b)* spectrum sharing between two geostationary earth orbit (GEO) satellite communication systems, and *c)* spectrum sharing between the GEO satellite communication system and the non-geosynchronous orbit (NGEO) communication system.

In the first category, the satellite communication system or the terrestrial communication system can be considered the primary system, and the other one is considered the secondary system. The primary system can use spectrum resources without any constraint while the secondary system should use the same spectrum resources without significantly affecting the primary system. In [6]–[9], power control was applied in the secondary system to satisfy the interference constraints imposed by the primary system. In [10] and [11], the minimum separation distance between satellite earth

The associate editor coordinating the review of this manuscript and approving it for publication was Rongbo Zhu.

stations and terrestrial stations/terminals was analyzed. In [12] and [13], the beam control and beamforming techniques were adopted respectively to maximize the signal to interference plus noise ratio (SINR) towards the desired secondary system and to minimize the interference towards the primary system. In the secondary category, spectrum sharing between broadcasting satellite service (BSS) feeder links and fixed satellite service (FSS) downlinks can be based on a simple coordination mechanism by defining cognitive (protection) zones around the BSS stations [14]–[16] or a beam-hopping (BH) scheme [17]. In [18], a BH scheme-based dual satellite coexistence scenario was proposed, in which the power control method and the exclusion zone method were applied to avoid producing harmful interference to the primary system. In the last category, the in-line interference between a GEO satellite and a LEO satellite occurs in low latitudes. In [19], the effect of NGEO interference on the bit error rate of a GEO system was studied. In [20], in-line interference mitigation techniques for ensuring the coexistence of GEO and medium earth orbit (MEO) O3b satellite systems were studied in the uplink and downlink. The authors proposed an adaptive power control (APC) technique for NGEO transmissions in order to mitigate interference. In [21], the authors also use APC technology to reduce the interference between GEO and LEO satellites. In [22], as a part of the wireless multimedia sensor networks (WMSNs), the LEO satellite system shares spectrum resources with the GEO satellite system by dynamic frequency allocation and setting a keep-out region. In [23], the in-line interference was mitigated by tilting the direction normal of phased array antennas of LEO satellites.

The LEO satellite constellation system shares spectrum with the GEO high throughput satellite communication system in Ka-band is what we are interested in. As mentioned before, the in-line interference between GEO satellites and LEO satellites is inevitable in low latitudes. OneWeb has proposed a progressive satellite pitch adjustment maneuver, 16 highly-elliptical user beams can be selectively switched off when in-line events occur [3]. While SpaceX and Telesat rely on steerable and shapeable beams to keep a minimum angular separation between GEO and LEO satellite beams. All of these systems adopt multibeam schemes in the downlink case but [24], [25] have proved that the BH scheme, to some degree, is more suitable for LEO satellite constellation systems. Our research focuses on resource allocation (RA) where the LEO satellite constellation system with the BH scheme shares the spectrum of the GEO satellite system with the multibeam scheme. As far as we know, related researches are rare. Wang *et al.* [21] proposed a novel dual satellite coexistence network that took the LEO satellite system as the primary system with the multibeam scheme and took the GEO satellite system as the secondary system with the BH scheme. However, [21] did not consider the traffic demand distribution. Sharma *et al.* [18] presented cognitive BH for spectral coexistence of two GEO multibeam satellites, and they did not consider the traffic demand distribution too.

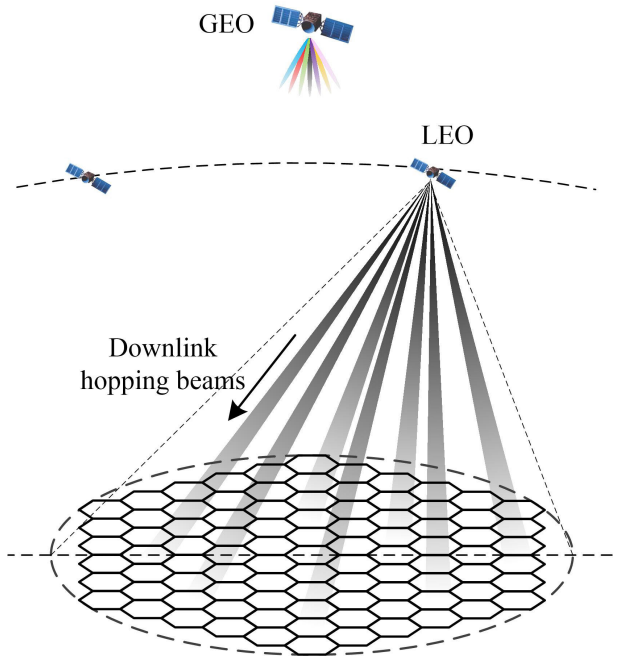


**FIGURE 1.** Spectrum sharing scenario of the GEO and LEO satellite systems in the downlink.

Zuo *et al.* [17] presented two 4-D (time, frequency, power, and dedicated spot beam) RA schemes in the cognitive satellite system, but it was not in the GEO/LEO scenario.

In this paper, an LEO satellite constellation system is considered as a secondary system to share the spectrum resources of a GEO high throughput satellite communication system. When the LEO satellite is in low latitude, its frequency bands and transmitting power are limited in order not to interfere with the GEO satellite. Conventional LEO multibeam satellites have poor adaptability in this scenario especially when the traffic demand is unevenly distributed. Compared with conventional LEO multibeam satellites, LEO BH satellites are less limited in the time dimension and therefore LEO BH satellites can adapt to the uneven distribution of traffic demand by adjusting the timeslot allocation. We also propose a RA algorithm for LEO BH satellites to minimize the variance between the traffic demand and the traffic supply.

The rest of this paper is organized as follows: Section II describes the LEO satellite constellation system model and the GEO high throughput satellite system model. The interference between the GEO satellite and the LEO satellite is also analyzed in this section. In Section III, the RA algorithm for LEO BH satellites is proposed. Section IV presents and analyzes the simulation results. Section V concludes this paper.

## II. GEO/LEO SATELLITE SYSTEMS SPECTRUM SHARING MODEL

### A. SPECTRUM SHARING SCENARIO

This paper considers a LEO satellite constellation system operating at polar orbits. It is assumed that there is a GEO

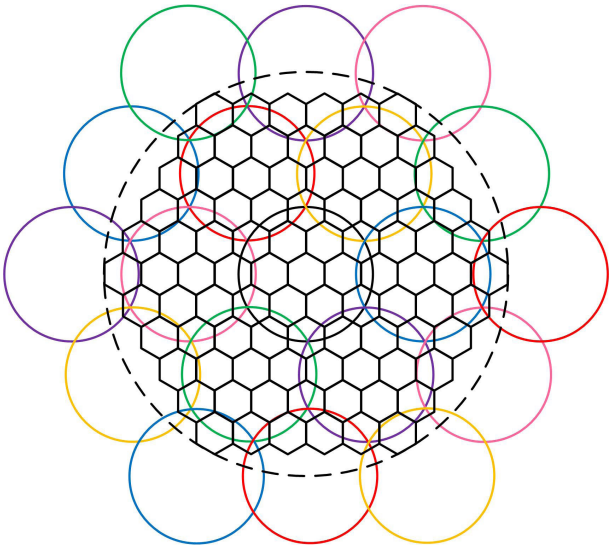

**FIGURE 2.** Spectrum distribution on the LEO satellite coverage area under multibeam coverage of the GEO satellite.

high throughput satellite that is above one of the orbits of the LEO satellite constellation system. As shown in Fig. 1, the GEO satellite system is served as the primary system which adopts multibeam coverage mode paired with frequency reuse. LEO satellite coverage areas are in fixed positions, which is beneficial for coverage areas to sense or predict the spectrum of the GEO satellite. Each coverage area is served by an LEO satellite. Correspondingly, LEO satellites are equipped with phased array antennas, which can form spotbeams with staring ability. A coverage area consists of many subareas which are called cells in this paper, and these cells are illuminated by LEO satellites' spotbeams in the BH manner. As the secondary system, the LEO satellite constellation system shares the spectrum of the GEO satellite system in the downlink, and the in-line interference occurs in low latitudes. In order to avoid harmful interference to the primary system, the transmitting power, frequency band usage, and illuminated beams of the LEO satellite will be strictly limited. In this scenario, it is meaningful to optimize the RA of the LEO satellite constellation system.

We assume that a hexagonal LEO satellite coverage area and the spectrum distribution caused by a GEO satellite on the coverage area are shown in Fig. 2 without loss of generality. Let $N_c$ denotes the cell number of the coverage area; $R_g$ and $R_l$ denote the beam coverage radius of the GEO satellite system and the cell radius (equals to the spotbeam coverage radius) of the LEO satellite system respectively; $H_g$ denotes the orbit height of the GEO satellite, and it is equal to 35786km; $H_l$ denotes the orbit height of LEO satellite; $\left(S_g^{lon}, 0\right)$ denotes the longitude and latitude of the GEO satellite; $\left(S_{l(t)}^{lon}, S_{l(t)}^{lat}\right)$ denotes the longitude and latitude of the LEO satellite at time $t$; $\left(C_{l,i}^{lon}, C_{l,i}^{lat}\right)$ denotes the longitude and latitude of the $i$th cell's center of the coverage area; $\left(C_{g,j}^{lon}, C_{g,j}^{lat}\right)$ denotes the longitude and latitude of the th beam's center of the GEO satellite; $B_{tot}$ denotes the shared spectrum, which is divided into $F_u$ sub-bands $\{f_1, f_2, \ldots, f_{F_u}\}$, and $F_u$ denotes the frequency reuse factor of the GEO satellite system.

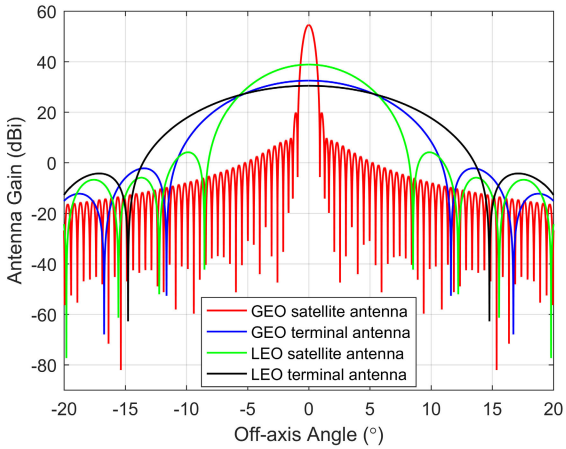


**FIGURE 3.** Antenna radiation patterns for satellites and terrestrial terminals.

### B. ANTENNA MODEL

Antenna radiation patterns are vital in interference analysis and simulation experiments. The ITU (International Telecommunication Union) has issued recommendations about antenna radiation patterns of satellites and earth stations for frequency coordination and interference assessment. They are ITU-R S.465-6 [26], ITU-R S.672-4 [27], ITU-R S.1428-1 [28], and ITU-R S.1528 [29]. But we adopt a unified antenna radiation pattern [18] for satellites and terrestrial terminals without loss of generality. In our simulations, the unified antenna radiation pattern is given by:

$$G(\theta) = G_0 \left[ \frac{J_1(u(\theta))}{2u(\theta)} + 36 \frac{J_3(u(\theta))}{u(\theta)^3} \right], \tag{1}$$

where $\theta$ is the off-axis angle; $G_0$ is the peak beam gain defined as $G_0 = \eta N^2 \pi^2 / \theta_{3dB}^2$; $\eta$ is the antenna efficiency generally equal to 0.7; $N$ is a constant related to the field distribution of antenna radiation pattern, equal to 65 in this paper; $\theta_{3dB}$ is the 3dB gain angle of the antenna; $J_1(\cdot)$ and $J_3(\cdot)$ represent the Bessel function of the first kind and the third kind respectively; $u(\theta) = 2.07123 \sin\theta / \sin\theta_{3dB}$.

The 3dB gain angle of the GEO/LEO satellite transmitting antenna $\theta_{3dB}^{*,s,t}$ is calculated by:

$$\theta_{3dB}^{*,s,t} = \frac{180^\circ}{\pi} \arctan\left(\frac{R_*}{H_*}\right), \tag{2}$$

where $* = g$ represents GEO satellites and $* = l$ represents LEO satellites. The 3dB gain angles of GEO and LEO terrestrial terminal receiving antennas are represented by $\theta_{3dB}^{g,e,r}$ and $\theta_{3dB}^{l,e,r}$ respectively. Once the 3dB gain angle is given, the antenna radiation pattern is determined according to function (1). Fig. 3 shows the antenna radiation patterns for satellites and terrestrial terminals in our simulations.

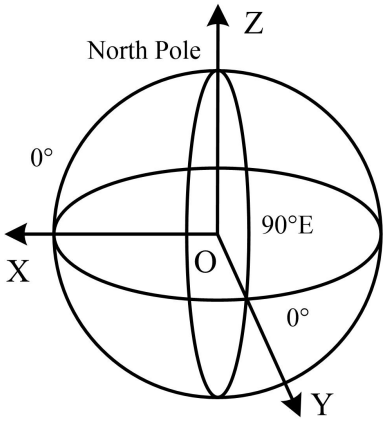


**FIGURE 4.** The diagram of the spatial rectangular coordinate system.

### C. INTERFERENCE MODEL

For the convenience of calculation, we establish a spatial rectangular coordinate system that takes the center of the earth as the coordinate origin, takes the direction from the center of the earth to the intersection of the equator and the prime meridian as the direction of the X-axis, takes the direction from the center of the earth to the intersection of the equator and the longitude 90°E as the direction of the Y-axis, and takes the direction from the center of the earth to the north pole as the direction of the Z-axis. As shown in fig. 4. Then the transformation from geographical coordinates to spatial rectangular coordinates is established, taking the LEO satellite geographical coordinate $\left(S^{lon}_{l(t)}, S^{lat}_{l(t)}\right)$ as an example, that is:

$$\begin{bmatrix} x^s_{l(t)} \\ y^s_{l(t)} \\ z^s_{l(t)} \end{bmatrix} = \begin{bmatrix} (R_e + H_l)\cos\left(S^{lon}_{l(t)}\right)\cos\left(S^{lat}_{l(t)}\right) \\ (-1)^a (R_e + H_l)\cos\left(S^{lon}_{l(t)}\right)\sin\left(S^{lat}_{l(t)}\right) \\ (-1)^b (R_e + H_l)\sin\left(S^{lon}_{l(t)}\right) \end{bmatrix}, \quad (3)$$

where $S_{l(t)} = \left(x^s_{l(t)}, y^s_{l(t)}, z^s_{l(t)}\right)$ is the spatial rectangular coordinate of the LEO satellite, $R_e$ denotes earth radius that equals 6371km, $a = 0$ or $a = 1$ when the LEO satellite is at east or west longitude, and $b = 0$ or $b = 1$ when the LEO satellite is at north or south longitude. Through the conversion formula similar to (3), we can convert geographic coordinates into spatial rectangular coordinates.

To avoid excessive interference to the GEO satellite system, the interference from LEO satellite beams to the GEO terrestrial terminals should be strictly limited. Let $I_{th}$ be the interference threshold level of the GEO satellite system to have sufficient protection. The interference power caused by each LEO satellite beam to GEO terrestrial terminals cannot exceed $I_{th}$. Let $S_g = \left(x^s_g, y^s_g, 0\right)$ be the spatial rectangular coordinates corresponding to $\left(S^{lon}_g, 0\right)$, similarly, $C_{g,i} = \left(x^c_{g,i}, y^c_{g,i}, z^c_{g,i}\right)$ corresponding to $\left(C^{lon}_{g,i}, C^{lat}_{g,i}\right)$, and $C_{l,i} = \left(x^c_{l,i}, y^c_{l,i}, z^c_{l,i}\right)$ corresponding to $\left(C^{lon}_{l,i}, C^{lat}_{l,i}\right)$.

The interference power $I^l_{i,\mathcal{E}}$ from a LEO satellite spotbeam serving cell $i$ to a GEO terrestrial terminal $\mathcal{E}$ located at $P_\mathcal{E} = (x_\mathcal{E}, y_\mathcal{E}, z_\mathcal{E})$ is given by:

$$I^l_{i,\mathcal{E}} = \xi^l_{i,\mathcal{E}} P^l_i G^l_t\left(\theta^l_{i,\mathcal{E}}\right) G^g_r\left(\theta^{g,l}_\mathcal{E}\right) L^l_\mathcal{E}, \quad (4)$$

where $\xi^l_{i,\mathcal{E}} \in \{0, 1\}$ indicates whether the frequency band used by the spotbeam serving cell $i$ overlaps with that used by the terrestrial terminal $\mathcal{E}$, $\xi^l_{i,\mathcal{E}} = 1$ means there is overlap, otherwise, $\xi^l_{i,\mathcal{E}} = 0$; $P^l_i$ denotes the power of beam serving cell $i$; $G^l_t(\cdot)$ denotes the transmitting antenna radiation pattern of LEO satellite beams; $G^g_r(\cdot)$ denotes the receiving antenna radiation pattern of GEO terrestrial terminals; $\theta^l_{i,\mathcal{E}} = \arccos\left[\left(\overrightarrow{S_{l(t)}C_{l,i}} \cdot \overrightarrow{S_{l(t)}P_\mathcal{E}}\right) / \left(\left|\overrightarrow{S_{l(t)}C_{l,i}}\right| \cdot \left|\overrightarrow{S_{l(t)}P_\mathcal{E}}\right|\right)\right]$ denotes the off-axis angle of the LEO satellite antenna from the beam serving cell $i$ to the GEO terrestrial terminal $\mathcal{E}$; $\theta^{g,l}_\mathcal{E} = \arccos\left[\left(\overrightarrow{P_\mathcal{E}S_g} \cdot \overrightarrow{P_\mathcal{E}S_{l(t)}}\right) / \left(\left|\overrightarrow{P_\mathcal{E}S_g}\right| \cdot \left|\overrightarrow{P_\mathcal{E}S_{l(t)}}\right|\right)\right]$ denotes the off-axis angle of the GEO terrestrial terminal $\mathcal{E}$ from the GEO satellite to the LEO satellite[1]; and $L^l_\mathcal{E}$ denotes the free space propagation loss from the LEO satellite to the GEO terrestrial terminal $\mathcal{E}$. $L^l_\mathcal{E}$ is given by:

$$L^l_\mathcal{E} = \left(\frac{4\pi d^l_\mathcal{E}}{\lambda}\right), \quad (5)$$

where $d^l_\mathcal{E}$ is the distance between the LEO satellite and the GEO terrestrial terminal $\mathcal{E}$, $\lambda$ is the carrier wavelength.

We also have to consider the interference power caused by GEO satellite beams to cells (Cells are small enough to think that all LEO terrestrial terminals in a cell are in the same position). The interference power $I^g_{j,i}$ from the $j$th GEO satellite beam to the $i$th cell located at $\left(x^c_{l,i}, y^c_{l,i}, z^c_{l,i}\right)$ is given by:

$$I^g_{j,i} = \xi^g_{j,i} P^g_j G^g_t\left(\theta^g_{j,i}\right) G^g_r\left(\theta^{l,g}_i\right) L^g_i, \quad (6)$$

where $\xi^g_{j,i} \in \{0, 1\}$ indicates whether the frequency band used by the th GEO satellite beam overlaps with that used by the $i$th cell, $\xi^g_{j,i} = 1$ means there is overlap, otherwise, $\xi^g_{j,i} = 0$; $P^g_j$ denotes the power of the $j$th GEO satellite beam; $G^g_t(\cdot)$ denotes the transmitting antenna radiation pattern of GEO satellite beams; $G^l_r(\cdot)$ denotes the receiving antenna radiation pattern of LEO terrestrial terminals; $\theta^g_{j,i} = \arccos\left[\left(\overrightarrow{S_gC_{g,j}} \cdot \overrightarrow{S_gC_{l,i}}\right) / \left(\left|\overrightarrow{S_gC_{g,j}}\right| \cdot \left|\overrightarrow{S_gC_{l,i}}\right|\right)\right]$ denotes the off-axis angle of the GEO satellite antenna from the $j$th GEO satellite beam to the $i$th cell; $\theta^{l,g}_i = \arccos\left[\left(\overrightarrow{C_{l,i}S_{l(t)}} \cdot \overrightarrow{C_{l,i}S_g}\right) / \left(\left|\overrightarrow{C_{l,i}S_{l(t)}}\right| \cdot \left|\overrightarrow{C_{l,i}S_g}\right|\right)\right]$ denotes the off-axis angle of the LEO terrestrial terminal from the LEO satellite to the GEO satellite, and $L^g_i$ denotes the free space propagation loss from the GEO satellite to

[1]It is reasonable to think that the receiving antenna of GEO terrestrial terminals is facing the GEO satellite, similarly, the receiving antenna of LEO terrestrial terminals is facing the LEO satellite.

the $i$th cell. $L_i^g$ is given by:

$$L_i^g = \left(\frac{4\pi d_i^g}{\lambda}\right), \tag{7}$$

where $d_i^g$ is the distance between the GEO satellite and the $i$th cell.

## III. RESOURCE ALLOCATION

As the secondary system, the LEO satellite constellation system optimizes RA to satisfy the traffic demand of cells under the condition of limited frequency bands and transmitting power, which has practical significance. In this paper, our goal of RA is to minimize the variance between the traffic demand of cells and the traffic supply of the LEO BH satellite, that is:

$$\min \sum_{i=1}^{N_c} (\mathcal{D}_i - \mathcal{S}_i)^2, \tag{8}$$

where $\mathcal{D}_i$ and $\mathcal{S}_i$ denote the traffic demand of cell $i$ and the traffic supply of the LEO BH satellite to the cell $i$ respectively. The resources allocated to cells by the LEO BH satellite include frequency bands, transmitting power, illuminated beams, and timeslots. Unfortunately, the allocation of these four resources is coupled and it is difficult to obtain a globally optimal solution of (8). To deal with it, the RA problem can be decomposed into three sub-problems, namely, frequency bands selection (FBS) problem, illuminated cell selection (ICS) problem, and transmitting power allocation (TPA) problem. In particular, timeslots allocation is integrated into the process of RA and is not calculated separately. We solve each sub-problem in order and finally form a complete RA scheme.

### A. THE FBS PHASE

In our system, each LEO satellite spotbeam has a single carrier that occupies one sub-band or several continuous sub-bands as broadband to avoid the back-off of the amplifier and the guard interval of the bandwidth. During the FBS phase, the total transmitting power $P_{tot}$ of the LEO satellite is evenly divided into $N_b$ LEO satellite spotbeams, which means that the maximum transmitting power over each LEO satellite spotbeam should not exceed $P_{tot}/N_b$. Selecting the appropriate bandwidth and quasi transmitting power[2] to maximize the transmission capacity for each cell is the problem that the FBS solves. The quasi transmission capacity $\hat{C}_i^l$ based on Shannon's capacity is given by:

$$\hat{C}_i^l = B_i^l \log_2\left(1 + \frac{\alpha_i^l \hat{P}_i^l}{n_0 B_i^l + I_{tot}^g}\right), \tag{9}$$

where $B_i^l$ and $\hat{P}_i^l$ denote the bandwidth and quasi transmitting power respectively for the $i$th cell; $\alpha_i^l$ denotes the channel coefficient from the LEO satellite to the $i$th cell; $n_0$ denotes the power spectral density of noise; $I_{tot,i}^g$ denotes the total interference power that cell $i$ receive from the GEO satellite, and $I_{tot,i}^g$ is given by:

$$I_{tot,i}^g = \sum_j I_{j,i}^g. \tag{10}$$

In section II, we obtain the interference power $I_{i,\mathcal{E}}^l$, and $I_{i,\mathcal{E}}^l \leqslant I_{th}$ for protecting the GEO satellite system. For sub-band $f_k$, $k = 1, 2, \ldots, F_u$, there is:

$$P_{i,f_k}^l \leqslant \frac{I_{th}}{\beta_{i,f_k}}, \tag{11}$$

where $P_{i,f_k}^l$ is the maximum transmitting power when only the sub-band $f_k$ is used in the spotbeam serving cell $i$, $\beta_{i,f_k} = \max_{\mathcal{E}} \left\{\xi_{i,\mathcal{E}}^l G_t^l\left(\theta_{i,\mathcal{E}}^l\right) G_r^g\left(\theta_{\mathcal{E}}^{g,l}\right) L_{\mathcal{E}}^l\right\}$. Hence, we can obtain the corresponding relationship between a sub-band and the maximum transmitting power using the sub-band by (11). The FBS problem can be modeled as:

$$\max_{B_i^l, \hat{P}_i^l} \ \hat{C}_i^l, \quad \forall i \tag{12a}$$

$$s.t.\ B_i^l \subseteq \{f_1, \ldots, f_{F_u}\} \tag{12b}$$

$$\hat{P}_i^l \leqslant P_{tot}/N_b, \quad \forall f_k \in B_i^l \tag{12c}$$

$$\hat{P}_i^l \leqslant P_{i,f_k}^l, \quad \forall f_k \in B_i^l \tag{12d}$$

This is a simple non-linear programming problem, and it can be solved quickly when the frequency reuse factor $F_u$ is a small integer, such as 4, 7, 9, 11, etc. The FBS algorithm that selects the appropriate broadband for a cell $i$ is shown in Algorithm 1.

An example is shown in Fig. 5. The shared spectrum is divided into 7 sub-bands from $f1$ to $f7$ (It is worth noting that the bandwidth of sub-bands can be different). The maximum transmitting power over each sub-band is given from $p1$ to $p7$ for a cell $x$. $p0 = P_{tot}/N_b$. Since the cell $x$ achieves maximum transmission capacity when $B_x^l = \{f2, f3, f4, f5\}$ and $P_x^l = p4$, then $\{f2, f3, f4, f5\}$ should be selected as the broadband when the cell $x$ is served and $p4$ is the quasi transmitting power.

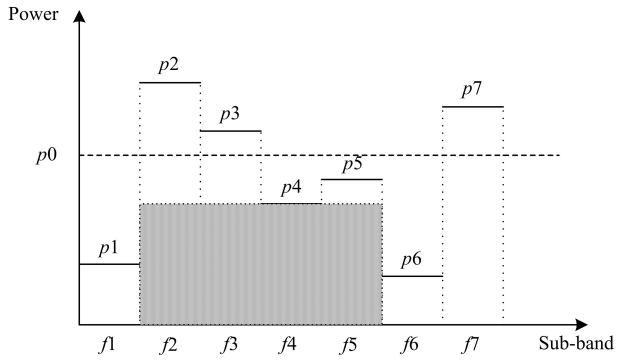


**FIGURE 5.** An example of the FBS.

[2]The quasi transmitting power calculated in the FBS phase is not the final transmitting power, which will be calculated in the TPA phase.

**Algorithm 1** The FBS Algorithm

**Input:** $P_{tot}, B_{tot}, f_1, \ldots, f_{F_u}, N_b, \left\{P^l_{i,f_k}\right\}, \{\alpha^l_i\}, \left\{I^g_{tot,i}\right\}$.
**Output:** Broadband set $\left\{B^l_i\right\}$, quasi transmitting power set $\left\{\hat{P}^l_i\right\}$, and quasi transmission capacity set $\left\{\hat{C}^l_i\right\}$.
**Begin:**

1: **for** $i$=1 to $N_c$ **do**
2: Initialize $\mathcal{B} = \{f_1, \ldots, f_{F_u}\}$, $C_{\max}$=0, $B^l_i = 0$.
3: **while** true **do**
4: **if** $\mathcal{B} = \varnothing$ **then**
5: Go to step 24.
6: **end if**
7: $f_x = \underset{f_k \in \mathcal{B}}{arg\min} \left\{P^l_{i,f_k}\right\}$.
8: $P = \min\limits_{f_k \in \mathcal{B}} \left\{P^l_{i,f_k}\right\}$.
9: **if** $P \geqslant P_{tot}/N_b$ **then**
10: Find the maximum continuous broadband $B_{\max}$ from $\mathcal{B}$, $B = B_{\max}$.
11: Calculate $C$ by (9).
12: **if** $C > C_{\max}$ **then**
13: $B^l_i = B$, $\hat{P}^l_i = P_{tot}/N_b$, $\hat{C}^l_i = C$.
14: Go to step 24.
15: **end if**
16: **end if**
17: Find the maximum continuous broadband $B_{\max}$ from $\mathcal{B}$, $B = B_{\max}$.
18: Calculate $C$ by (9).
19: **if** $C > C_{\max}$ **then**
20: $B^l_i = B$, $\hat{P}^l_i = P_{tot}/N_b$, $\hat{C}^l_i = C$.
21: **end if**
22: Remove $f_x$ from $\mathcal{B}$.
23: $P^l_{i,f_x} = P_{tot}/N_b$.
24: **end while**
25: **end for**

**End**
**Return:** $\left\{B^l_i\right\}, \left\{\hat{P}^l_i\right\}, \left\{\hat{C}^l_i\right\}$.

### B. THE ICS PHASE

In the LEO satellite constellation system, the cycle of downlink transmission is $T_c$, which mainly consists of two parts. One is the RA-related part, which includes channel state information (CSI) collection, RA calculation, broadcasting RA results, etc. the other is called the BH time window. As shown in Fig. 6. A BH time window consists of $N_{ts}$ timeslots and the duration of a timeslot is $T_s = T_w/N_{ts}$. In each timeslot, at most $N_b$ cells are illuminated, where $N_b$ is the total spotbeam number of the LEO BH satellite.

In the FBS phase, there is a high probability that the available broadband between cells will overlap. To avoid the co-channel interference (CCI) between adjacent cells, an interference distance threshold $D_{th}$ is set, which means that the distance of any two cells illuminated at the same time should be longer than $D_{th}$. It is noted that $D_{th}$ determines the spatial multiplexing of LEO BH satellites and we choose an appropriate value $D_{th}$ to achieve the tradeoff between spatial multiplexing and CCI.

**Algorithm 2** The ICS Algorithm

**Input:** $\{N_i\}$.
**Output:** The set of illuminated cells $\Phi$.
**Begin:**

1: Initialize $\Phi = \varnothing$, $Count = 0$.
2: Sort $\{N_i\}$ in descending order, get a new list $\left\{N_{i,j}\right\}$.
3: **for** $j$=1 to $N_c$ **do**
4: **if** $Count = N_c$ or $N_{i,j} = 0$ **then**
5: Go to step 10.
6: **end if**
7: **if** $\min_{v \in \Phi} d_{i,v} \geqslant D_{th}$ **then**
8: Add $i$ to $\Phi$, $Count = Count + 1$.
9: **end if**
10: **end for**

**End**
**Return:** $\Phi$.

Although the LEO BH satellite is limited in the frequency and power dimension, it is relatively loose in the time dimension. We take advantage of the flexibility of BH satellites in the time dimension to make the satellite resource incline to the cells with large traffic demand or low transmission capacity by allocating more timeslots to them. The cell with low transmission capacity usually needs more timeslots to satisfy its traffic demand. Hence, our ICS strategy is to give priority to the cell which needs the greatest number of timeslots. Let $d_{i,m}$ be the remaining traffic demand of the $i$th cell in the $m$th timeslot, there is:

$$N_i = \lceil \frac{d_{i,m}}{\hat{C}^l_i T_s} \rceil, \tag{13}$$

where $N_i$ denotes the number of timeslots needed for the $i$th cell; $\hat{C}^l_i$ denotes the quasi transmission capacity of the $i$th cell which is calculated in the FBS phase; $\lceil \cdot \rceil$ represents rounding up operation. In every timeslot, the cells are selected to be illuminated in turn according to the descending order of the number of timeslots needed by each cell. If the distance between a cell and any one of the previously selected cells is less than $D_{th}$, skip this cell and consider the next cell until one of the following three situations: *a)* $N_b$ cells are selected; *b)* no cell needs a transmission; *c)* there is no cell can be illuminated due to the constraint of interference distance threshold $D_{th}$. The ICS algorithm that selects the illuminated cells in a timeslot is summarized in Algorithm 2. In a BH time window, the timeslot allocation pattern is similar to that shown in Fig. 6. In the first several timeslots, cells with the largest timeslot demand will be selected continuously. And adjacent cells cannot be illuminated at the same timeslot.

### C. THE TPA PHASE

In the previous two phases, the total transmitting power $P_{tot}$ may not be sufficiently used. In the FBS phase, the quasi

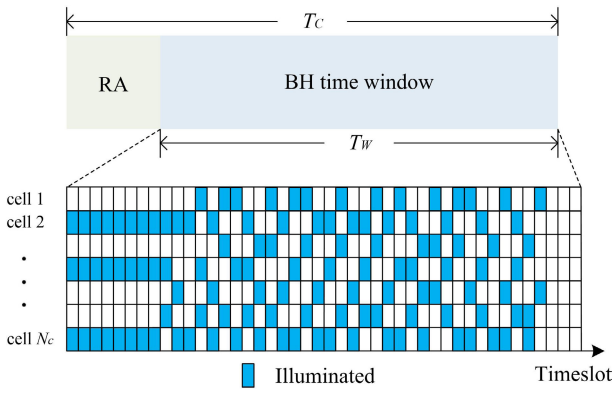


**FIGURE 6.** The downlink transmission cycle structure and the timeslot allocation pattern.

transmitting power of some cells may less than $P_{tot}/N_b$. In the ICS phase, the number of illuminated cells at the same timeslot may less than $N_b$. But in fact, the transmitting power of some cells can exceed $P_{tot}/N_b$ as long as it does not exceed the maximum transmitting power of the broadband that those cells use. In order to make full use of the total transmitting power, in the TPA phase, the transmitting power of the illuminated cells in the same timeslot should be adjusted. A simple and efficient method is to allocate unused power to cells by the water filling algorithm. Let $\tilde{N}_b$ denotes the number of illuminated cells in a timeslot, $\tilde{N}_b \leqslant N_b$; $\Phi$ denotes the set of illuminated cells in this timeslot; $P_{i,\max}$ denotes the maximum transmitting power of the broadband that the cell $i$ uses; and $P_{i,un}$ denotes the extra power allocated to the cell $i$, which comes from unused power $P_{un}$. The unused power $P_{un}$ in this timeslot is given by:

$$P_{un} = P_{tot} - \sum_{i\in\Phi} \hat{P}_i^l. \tag{14}$$

The TPA problem can be modeled as:

$$\max_{P_{i,un}} \sum_{i\in\Phi} C_i^l \tag{15a}$$

$$s.t.\ C_i^l = B_i^l \log_2 \left[1 + \frac{\alpha_i^l \left(\hat{P}_i^l + P_{i,un}\right)}{n_0 B_i^l + I_{tot,i}^g}\right], \quad \forall i \in \Phi \tag{15b}$$

$$\sum_{i\in\Phi} \left(\hat{P}_i^l + P_{i,un}\right) \leqslant P_{tot} \tag{15c}$$

$$0 \leqslant P_{i,un} \leqslant P_{i,\max} - \hat{P}_i, \quad \forall i \in \Phi \tag{15d}$$

where constraint (15c) indicates that the sum of transmitting power allocated for illuminated cells should be less than the total transmitting power provided by the LEO BH satellite; constraint (15d) indicates that the transmitting power allocated for an illuminated cell should not be lower than the quasi transmitting power of this cell, nor higher than the maximum transmitting power of this cell.

We don't consider constraint (15d) for the moment, and the TPA problem is convex. Constructing the Lagrangian function as (without constraint (15d)):

$$\mathcal{L}\left(P_{i,un}\right) = \sum_{i\in\Phi} B_i^l \log_2 \left[1 + \frac{\alpha_i^l \left(\hat{P}_i^l + P_{i,un}\right)}{n_0 B_i^l + I_{tot,i}^g}\right] + \rho \left[P_{tot} - \sum_{i\in\Phi} \left(\hat{P}_i^l + P_{i,un}\right)\right], \tag{16}$$

where $\rho$ is a Lagrange multiplier. Differentiating with respect to $P_{i,un}$, we have the optimum $P_{i,un}$, which satisfies:

$$\hat{P}_i^l + P_{i,un} = \frac{B_i^l}{\rho \ln 2} - \frac{n_0 B_i^l + I_{tot,i}^g}{\alpha_i^l}. \tag{17}$$

Let $\sum_{i\in\Phi} \left(\hat{P}_i^l + P_{i,un}\right) = P_{tot}$, there is:

$$\rho = \frac{\sum_{i\in\Phi} B_i^l}{\ln 2 \cdot \left(P_{tot} + \sum_{i\in\Phi} \frac{n_0 B_i^l + I_{tot,i}^g}{\alpha_i^l}\right)}. \tag{18}$$

Substituting (18) into (17), we obtain:

$$P_{i,un} = \frac{B_i^l}{\sum_{i\in\Phi} B_i^l} \left(P_{tot} + \sum_{i\in\Phi} \frac{n_0 B_i^l + I_{tot,i}^g}{\alpha_i^l}\right) - \frac{n_0 B_i^l + I_{tot,i}^g}{\alpha_i^l} - \hat{P}_i^l. \tag{19}$$

**Algorithm 3** The TPA Algorithm

**Input:** $\Phi$, $P_{tot}$, $\{\alpha_i^l\}$, $\{B_i^l\}$, $\left\{\hat{P}_i^l\right\}$, $\left\{P_{i,\max}^l\right\}$, $\left\{I_{tot,i}^g\right\}$.
**Output:** The extra power allocated to illuminated cells $\left\{P_{i,un}\right\}$.
**Begin:**
1: Initialize $\Lambda = \varnothing$, $P = P_{tot}$.
2: **while** $\Phi \neq \varnothing$ **do**
3: $P_{tot} = P - \sum_{j\in\Lambda} \left(\hat{P}_j^l + P_{j,un}\right)$.
4: Calculate $P_{i,un}$ by (19).
5: **if** $0 \leqslant P_{i,un} \leqslant P_{i,\max} - \hat{P}_i$ for $\forall i \in \Phi$ **then**
6: Go to step 20.
7: **else if** $P_{i,un} \geqslant 0$ for $\forall i \in \Phi$ **then**
8: **if** $P_{i,un} > P_{i,\max} - \hat{P}_i$ **then**
9: $P_{i,un} = P_{i,\max} - \hat{P}_i$.
10: Remove $i$ from $\Phi$.
11: Add $i$ to $\Lambda$.
12: **end if**
13: **else**
14: **if** $P_{i,un} < 0$ **then**
15: $P_{i,un} = 0$.
16: Remove $i$ from $\Phi$.
17: Add $i$ to $\Lambda$.
18: **end if**
19: **end if**
20: **end while**
**End**
**Return:** $\left\{P_{i,un}\right\}$.

**Algorithm 4** The RA Algorithm

**Input:** $P_{tot}, B_{tot}, f_1, \ldots, f_{F_u}, N_b, \left\{P^l_{i,f_k}\right\}, \{\alpha^l_i\}, \left\{I^g_{tot,i}\right\}, \{N_i\}$.
**Output:** A RA scheme.
**Begin:**

1: **for** $m$=1 to $N_{ts}$ **do**
2: The FBS algorithm calculates $\left\{B^l_i\right\}$, $\left\{\hat{P}^l_i\right\}$, $\left\{\hat{C}^l_i\right\}$, and $\left\{P^l_{i,\max}\right\}$.
3: The ICS algorithm gets $\Phi$.
4: The TPA algorithm calculates $\left\{P_{i,un}\right\}$.
5: In the $m$th timeslot, the illuminated cells are included in $\Phi$, the bandwidth for cell $i$ is $\hat{P}^l_i + P_{i,un}$, the transmitting power for cell $i$ is $\hat{P}^l_i + P_{i,un}$, and $i \in \Phi$.
6: **end for**

**End**
**Return:** A RA scheme.

Now we take constraint (15d) into consideration, and an iterative method is summarized in Algorithm 3 to make $P_{i,un}$ satisfy constraint (15d) without losing the optimal result.

### D. RA SCHEME FOR A TRANSMISSION CYCLE

Through the three phases of FBS, ICS, and TPA, the LEO BH satellite resources are allocated to cells at the timeslot-level. To form a RA scheme for a transmission cycle, the following two reasonable assumptions should be accepted due to the duration of a transmission cycle is short enough: *a)* the LEO satellite is stationary within a transmission cycle; *b)* the channel state is constant within a transmission cycle. In the RA-related part of a transmission cycle, the LEO satellite constellation system firstly collects CSI reported from cells and calculates the traffic amount that should be transmitted to each cell, then executes the RA algorithm, and finally broadcasts the result of RA to all cells. The RA algorithm is summarized in Algorithm 4 which includes the FBS algorithm, the ICS algorithm, and the TPA algorithm in it.

## IV. NUMERICAL RESULTS

In this section, the RA performance of the LEO satellite constellation system we proposed in the scenario of sharing spectrum with the GEO satellite system is presented. As a comparison, another LEO multibeam satellite system, which adopts the APC technology in the scenario of sharing spectrum with the GEO satellite system, as defined in [20], is presented as a benchmark system. The hexagonal LEO satellite coverage area, the cell distribution, and part of the GEO satellite's beam distribution are shown in Fig.2. The GEO Satellite generates multibeam coverage with 7-color multiplexing, and all GEO satellite beams have the same power and bandwidth. We let each cell generate random traffic demand over time. All the traffic arriving at the LEO satellite will be temporarily stored in the queue of the LEO satellite transponder waiting to be sent. At the same time, in order to avoid congestion caused by excessive traffic, the traffic waiting for more than $T_q$ will be discarded. For simplicity, the proportion of the BH time window in the downlink transmission cycle is 100%, that is $T_c = T_w$. We carry out simulations in real-time within the time when the LEO satellite passes over the coverage area. Simulation parameters are shown in TABLE 1.

**TABLE 1. Simulation parameters.**

| Parameter | Value | |
|---|---|---|
| Common parameter | | |
| Shared spectrum | 18.5-19.5GHz | |
| Noise temperature | 293K | |
| Longitude and latitude of the center point of the coverage area | (105°E, 0°) | |
| Simulation time | 139s | |
| GEO satellite system parameter | | |
| Satellite orbit height $H_g$ | 35786Km | |
| Satellite longitude $S^{lon}_g$ | 103°E | |
| Single beam radius $R_g$ | 200Km | |
| Single beam power $P^g_j$ | 10W | |
| Frequency reuse factor $F_u$ | 7 | |
| Interference threshold $I_{th}$ | -132.5dBW | |
| LEO satellite constellation system parameter | | |
| Beam pattern | BH | Multibeam |
| Satellite orbit height $H_l$ | 1000Km | |
| Satellite longitude $S^{lon}_l$ | 105°E | |
| Spotbeam number $N_c$ | 13 | 91 |
| Spotbeam radius $R_l$ | 52Km | |
| Spatial/Frequency reuse factor | 7 | |
| Interference distance threshold $D_{th}$ | 200Km | |
| A cycle of downlink transmission $T_c$ | 50ms | |
| Timeslot number of a BH time window $N_{ts}$ | 50 | |
| Maximum queuing time $T_q$ | 10s | |
| Satellite antenna parameter | | |
| Antenna efficiency $\eta$ | 0.7 | |
| Constant related to field distribution $N$ | 65 | |
| GEO satellite transmitting antenna half-power angle $\theta^{g,s,t}_{3dB}$ | 0.32° | |
| GEO terminals receiving antenna half-power angle $\theta^{g,e,r}_{3dB}$ | 4.05° | |
| LEO satellite transmitting antenna half-power angle $\theta^{l,s,t}_{3dB}$ | 2.98° | |
| LEO terminals receiving antenna half-power angle $\theta^{l,e,r}_{3dB}$ | 5.12° | |

The throughput performance is firstly tested, as shown in Fig. 7. When the traffic demand level is low, compared with the benchmark system, our proposed LEO BH satellite has higher throughput, which means the LEO BH satellite can effectively reduce the loss of throughput caused by the uneven distribution of traffic demand. When the traffic demand is

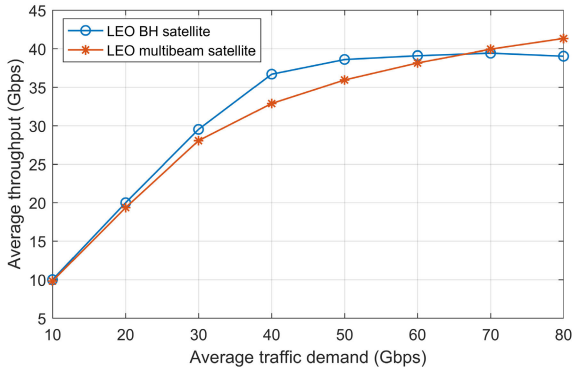


**FIGURE 7.** The throughput performance.

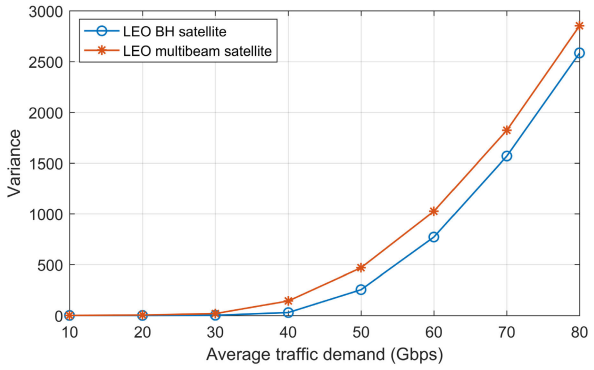


**FIGURE 8.** The variance between the traffic demand of cells and the traffic supply of the LEO satellite.

overloaded, the LEO BH satellite gradually loses the advantage of flexible RA, while for the benchmark system, all the beams can transmit with almost the maximum capacity. Hence, when the traffic demand is overloaded, the benchmark system has a higher throughput than the LEO BH satellite.

Fig. 8 shows the variance between the total traffic demand of cells and the total traffic supply provided by the LEO satellite to cells during the simulation time. No matter the traffic demand is at a low or high level, the LEO BH satellite always has a lower variance than the LEO multibeam satellite,

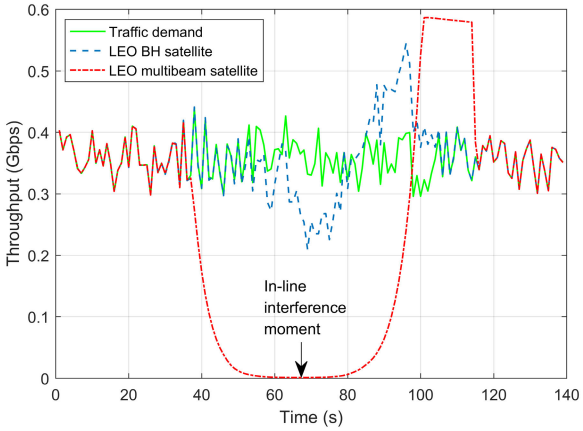


**FIGURE 10.** The throughput of a cell that will suffer in-line interference with the movement of the LEO satellite.

which means that the LEO BH satellite has better adaptability for uneven distribution of traffic demand. A more intuitive statistical result is shown in Fig. 9, in which the average traffic demand of the whole coverage area is set to 30Gbps. Fig. 9 shows the comparison of the total downlink traffic transmission of each cell between the two systems. As we can see, the LEO BH satellite will give priority to cells with large traffic demand but it will also lead to a small number of cells with small traffic demand that cannot be fully satisfied.

The throughput provided by the LEO satellite constellation system when the in-line interference occurs is an important index that people pay close attention to. The LEO BH satellite can make full use of the spectrum hole of the GEO satellite, avoid the interference frequency band, and provide uninterrupted communication service for the terrestrial terminal. In the process of the LEO satellite passing over the coverage area, the throughput provided by different LEO satellites to a cell that will suffer in-line interference is shown in Fig. 10. For the benchmark system, there is a long period that the communication of the cell is interrupted. In order to avoid harmful interference to the primary system, when the GEO satellite, the LEO satellite, and the cell are in-line, the APC algorithm

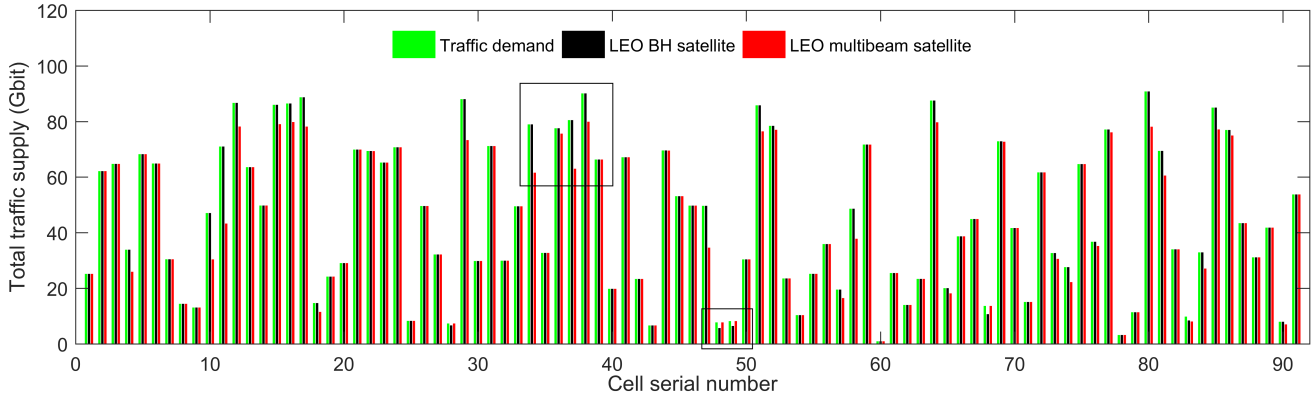


**FIGURE 9.** The total traffic demand and total traffic supply (Average traffic demand equals to 30Gbps).

of the benchmark system will reduce the transmitting power of the beam serving the cell to 0. For the LEO BH satellite, it can still serve the cell with relatively high throughput to ensure that the communication will not be interrupted when the in-line interference occurs.

## V. CONCLUSION

In this paper, the RA problem that LEO satellite constellation systems share a GEO high throughput satellite's spectrum is studied. Firstly, we build the downlink transmission model of the LEO BH satellite under a GEO multibeam satellite system. After setting up appropriate antenna models of satellite transmitting antennas and terrestrial terminal receiving antennas, the interference between the GEO multibeam satellite and the LEO BH satellite is analyzed. And then, to solve the RA problem of LEO BH satellite systems with limited frequency bands and transmitting power, this problem is decomposed into three sub-problems. We solve these three sub-problems in turn to complete the allocation of frequency bands, illuminated beams, and transmitting power. Finally, simulation results show that the LEO BH satellite system we proposed has good adaptability to the uneven distribution of traffic demand and can ensure that the communication between LEO satellites and ground terminals without interruption. Although the spectrum of the GEO satellite system is evenly divided and evenly distributed in this paper, our RA algorithm is also suitable for complex spectrum environments.

## REFERENCES

[1] S. Xia, Q. Jiang, C. Zou, and G. Li, "Beam coverage comparison of LEO satellite systems based on user diversification," *IEEE Access*, vol. 7, pp. 181656–181667, 2019.

[2] X. Qi, B. Zhang, and Z. Qiu, "A distributed survivable routing algorithm for mega-constellations with inclined orbits," *IEEE Access*, vol. 8, pp. 219199–219213, 2020.

[3] I. del Portillo, B. G. Cameron, and E. F. Crawley, "A technical comparison of three low Earth orbit satellite constellation systems to provide global broadband," *Acta Astronautica*, vol. 159, pp. 123–135, Jun. 2019.

[4] M. Höyhtyä, J. Kyröläinen, A. Hulkkonen, J. Ylitalo, and A. Roivainen, "Application of cognitive radio techniques to satellite communication," in *Proc. IEEE Int. Symp. Dyn. Spectr. Access Netw.*, Oct. 2012, pp. 540–551.

[5] S. Kandeepan, L. De Nardis, M.-G. Di Benedetto, A. Guidotti, and G. E. Corazza, "Cognitive satellite terrestrial radios," in *Proc. IEEE Global Telecommun. Conf. GLOBECOM*, Dec. 2010, pp. 1–6.

[6] E. Lagunas, S. Maleki, S. Chatzinotas, M. Soltanalian, A. I. Pérez-Neira, and B. Oftersten, "Power and rate allocation in cognitive satellite uplink networks," in *Proc. IEEE Int. Conf. Commun. (ICC)*, May 2016, pp. 1–6.

[7] S. Vassaki, M. I. Poulakis, A. D. Panagopoulos, and P. Constantinou, "Power allocation in cognitive satellite terrestrial networks with QoS constraints," *IEEE Commun. Lett.*, vol. 17, no. 7, pp. 1344–1347, Jul. 2013.

[8] S. Vassaki, M. I. Poulakis, and A. D. Panagopoulos, "Optimal iSINR-based power control for cognitive satellite terrestrial networks," *Trans. Emerg. Telecommun. Technol.*, vol. 28, no. 2, Feb. 2017, Art. no. e2945.

[9] J. Wang, D. Guo, B. Zhang, L. Jia, and X. Tong, "Spectrum access and power control for cognitive satellite communications: A game-theoretical learning approach," *IEEE Access*, vol. 7, pp. 164216–164228, 2019.

[10] D.-S. Oh, S.-M. Lee, D.-S. Ahn, and S. Kim, "A study on the separation distance for frequency sharing between GSO network and terrestrial network in ka band," in *Proc. VTC Spring IEEE Veh. Technol. Conf.*, May 2008, pp. 2967–2971.

[11] M. Höyhtyä, "Sharing FSS satellite c band with secondary small cells and D2D communications," in *Proc. IEEE Int. Conf. Commun. Workshop (ICCW)*, Jun. 2015, pp. 1606–1611.

[12] S. Tani, K. Motoyoshi, H. Sano, A. Okamura, H. Nishiyama, and N. Kato, "An adaptive beam control technique for Q band satellite to maximize diversity gain and mitigate interference to terrestrial networks," *IEEE Trans. Emerg. Topics Comput.*, vol. 7, no. 1, pp. 115–122, Jan. 2019.

[13] S. K. Sharma, S. Chatzinotas, and B. Ottersten, "Transmit beamforming for spectral coexistence of satellite and terrestrial networks," in *Proc. 8th Int. Conf. Cognit. Radio Oriented Wireless Netw.*, Jul. 2013, pp. 275–281.

[14] S. Maleki, S. Chatzinotas, B. Evans, K. Liolis, J. Grotz, A. Vanelli-Coralli, and N. Chuberre, "Cognitive spectrum utilization in ka band multibeam satellite communications," *IEEE Commun. Mag.*, vol. 53, no. 3, pp. 24–29, Mar. 2015.

[15] S. Maleki, S. Chatzinotas, J. Krause, K. Liolis, and B. Ottersten, "Cognitive zone for broadband satellite communications in 17.3–17.7 GHz band," *IEEE Wireless Commun. Lett.*, vol. 4, no. 3, pp. 305–308, Jun. 2015.

[16] M. Höyhtyä, "Frequency sharing between FSS and BSS satellites in the 17.3–18.4 GHz band," in *Proc. Adv. Wireless Opt. Commun. (RTUWO)*, Nov. 2015, pp. 176–179.

[17] P. Zuo, T. Peng, W. Linghu, and W. Wang, "Resource allocation for cognitive satellite communications downlink," *IEEE Access*, vol. 6, pp. 75192–75205, 2018.

[18] S. K. Sharma, S. Chatzinotas, and B. Ottersten, "Cognitive beamhopping for spectral coexistence of multibeam satellites," *Int. J. Satell. Commun. Netw.*, vol. 33, no. 1, pp. 69–91, Jan. 2015.

[19] C.-S. Park, C.-G. Kang, Y.-S. Choi, and C.-H. Oh, "Interference analysis of geostationary satellite networks in the presence of moving non-geostationary satellites," in *Proc. 2nd Int. Conf. Inf. Technol. Converg. Services*, Aug. 2010, pp. 1–5.

[20] S. K. Sharma, S. Chatzinotas, and B. Ottersten, "In-line interference mitigation techniques for spectral coexistence of GEO and NGEO satellites," *Int. J. Satell. Commun. Netw.*, vol. 34, no. 1, pp. 11–39, 2014.

[21] C. Wang, D. Bian, S. Shi, J. Xu, and G. Zhang, "A novel cognitive satellite network with GEO and LEO broadband systems in the downlink case," *IEEE Access*, vol. 6, pp. 25987–26000, 2018.

[22] C. Wang, D. Bian, G. Zhang, J. Cheng, and Y. Li, "A novel dynamic spectrum-sharing method for integrated wireless multimedia sensors and cognitive satellite networks," *Sensors*, vol. 18, no. 11, p. 3904, Nov. 2018.

[23] C. Zhang, J. Jin, H. Zhang, and T. Li, "Spectral coexistence between LEO and GEO satellites by optimizing direction normal of phased array antennas," *China Commun.*, vol. 15, no. 6, pp. 18–27, Jun. 2018.

[24] J. Lei and M. A. Vazquez-Castro, "Multibeam satellite frequency/time duality study and capacity optimization," *J. Commun. Netw.*, vol. 13, no. 5, pp. 472–480, Oct. 2011.

[25] J. Anzalchi, A. Couchman, P. Gabellini, G. Gallinaro, L. D'Agristina, N. Alagha, and P. Angeletti, "Beam hopping in multi-beam broadband satellite systems: System simulation and performance comparison with non-hopped systems," in *Proc. 5th Adv. Satell. Multimedia Syst. Conf. 11th Signal Process. Space Commun. Workshop*, Sep. 2010, pp. 248–255.

[26] *Reference Radiation Pattern for Earth Station Antennas in The Fixed-Satellite Service for Use in Coordination and Interference Assessment in The Frequency Range from 2 to 31GHz*, document ITU-R S.456-6, Jan. 2010.

[27] *Satellite Antenna Radiation Pattern for use as a Design Objective in the Fixed-Satellite Service Employing Geostationary Satellites*, document ITU-R S.672-4, May 2002.

[28] *Reference FSS Earth-Station Radiation Patterns for use in Interference Assessment Involving non-GSO Satellites in Frequency Bands Between 10.7 GHz and 30 GHz*, ITU-R S.1428-1m, Feb. 2001.

[29] *Satellite Antenna Radiation Patterns for Non-Geostationary Orbit Satellite Antennas Operating in the Fixed-Satellite Service Below 30 GHz*, documentITU-R S.1528, Jun. 2001.

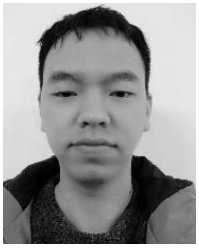

**JINGYU TANG** received the B.S. degree in telecommunications engineering from South China Normal University, China, in 2014, and the M.E. degree from the Army Engineering University of PLA, Nanjing, China, where he is currently pursuing the Ph.D. degree in communication engineering. His research interests include LEO satellite communications, dynamic resource management, and machine learning.

**DONGMING BIAN** received the Ph.D. degree from the PLA University of Science and Technology, Nanjing, China, in 2004. He is currently a Professor with the College of Communication Engineering, Army Engineering University of PLA, Nanjing. His research interests include wireless communications, satellite communications, and deep space communications.

**GUANGXIA LI** received the B.S. and M.S. degrees from the Institute of Communication Engineer, Nanjing, China, in 1983 and 1986, respectively. He is currently a Professor with the College of Communication Engineering, Army Engineering University of PLA, Nanjing. His current research interests include the design of communication systems, satellite communications, satellite navigation, communication anti-jamming, and satellite TT&C.

**JING HU** received the B.S. and M.S. degrees from the Nanjing University of Posts and Telecommunications, Nanjing, China, in 2003 and 2007, respectively. She is currently pursuing the Ph.D. degree with the College of Communications Engineering, Army Engineering University of PLA, Nanjing. Her current research interests include wireless communications, satellite communications, and communication anti-jamming.

**JIAN CHENG** received the Ph.D. degree from the PLA University of Science and Technology, Nanjing, China, in 2008. He is currently a Professor with the College of Communication Engineering, Army Engineering University of PLA, Nanjing. His research interests include satellite communications, satellite TT&C, and satellite covert communication.